Journal of Marine Research, 45, 667–698, 1987

Bomb radiocarbon in the Pacific: Annual and seasonal timescale variations

by Ellen R. M. Druffel[1]

ABSTRACT

Banded corals are used as proxy recorders of bomb radiocarbon in the surface of the Pacific Ocean. Bomb radiocarbon levels appeared to still be rising in the tropical Pacific by 1982, in contrast to temperate locations that peaked in the early 1970's. This is representative of the geostrophic transport of bomb-laden waters from higher latitudes toward the equator. The seasonal radiocarbon signal at Canton Island (3S, 172W) during the early 1970's was twice the amplitude of that at Fanning Island (4N, 159W), and the radiocarbon minima at these locations were offset by several months. The phase lag is caused primarily by the seasonally variant transequatorial Ekman transport, which funnels more upwelled, ^{14}C-poor water from summer to winter hemisphere. The seasonal variation of $\Delta^{14}C$ at Canton is larger because the peak input of ^{14}C-poor South Equatorial Current water is coincident with the period of greatest transequatorial Ekman transport to this region. Whereas, at the Fanning site, these inputs reach their maxima during opposing seasons, which causes a damping of the seasonal $\Delta^{14}C$ signal.

A time-stepped, multi-box model calculation is made to describe bomb radiocarbon distributions in the tropical Pacific, and hence to determine the influence of the South Equatorial Current flow on the chemistry of the central equatorial Pacific. The annual model results show that radiocarbon is influenced to a minor extent by this lateral flow, in agreement with previous studies. However, the seasonal version of the model reveals that the South Equatorial Current flow varies by a factor of 2–3 in order to explain the seasonal variations in bomb radiocarbon. Meridional geostrophic convergence and transequatorial Ekman transport from summer to winter hemisphere alone are not sufficient for defining the observed seasonal signals.

1. Introduction

Examination of bomb radiocarbon levels in surface ocean dissolved inorganic carbon (DIC) (Linick, 1978, 1980; Nydal and Loveseth, 1983; Ostlund and Stuiver, 1980), shows pronounced spatial variability in the $\Delta^{14}C$ values within major water masses. It is suspected that this inhomogeneity is caused by (1) seasonal changes in the flow field of the major current systems supplying the area and (2) seasonal changes in the depth of the mixed layer. From the GEOSECS results, Broecker and Peng (1980) noticed that surface waters in the temperate North Atlantic (20–35N) had $\Delta^{14}C$ values 35‰ higher in September 1972, just before late fall deepening of the mixed layer, than during March 1973 when the depth of the mixed layer was 200–400 m. They attributed the

1. Woods Hole Oceanographic Institution, Woods Hole, Massachusetts, 02543, U.S.A.

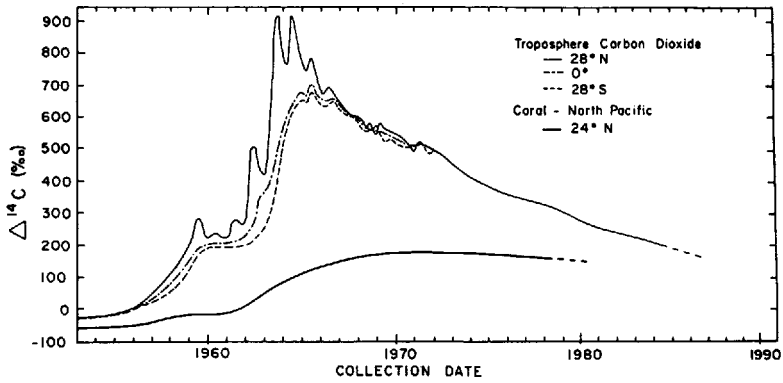

Figure 1. Time histories of bomb radiocarbon in atmospheric CO_2 from three latitudes (Nydal and Loveseth, 1983; Levin *et al.*, 1985) and in annual coral bands from French Frigate Shoals (see Fig. 3b).

difference to the concentration of atmospheric bomb $^{14}CO_2$ into the thinner summer mixed layer (100 m deep).

Evidence is presented of seasonal variation in bomb ^{14}C levels during the early 1970's in surface waters of the mid-tropical Pacific using banded corals as the data base. As winter mixing does not occur to any significant extent in tropical regions, an alternative explanation must be found for the seasonal variation observed in the bomb radiocarbon signal. Seasonal change in horizontal flow patterns of water in the tropical Pacific is the favored explanation.

Bomb radiocarbon was produced by stratospheric explosions of thermonuclear weapons in the 1950's and early 1960's and was introduced to the troposphere via the spring leak. Maximum $\Delta^{14}C$ values of 900–1000‰ were reached in northern hemisphere CO_2 by late 1963 (Nydal and Loveseth, 1983) and have since decreased to about 200‰ by 1983 (Levin *et al.*, 1985), mainly due to isotopic exchange with DIC in the oceans (Fig. 1). Pre-bomb $\Delta^{14}C$ values in the surface waters of the Pacific Ocean between 35N and 35S ranged from −75 to −40‰ (Druffel, 1985) in the early 1950's and rose to values that ranged from +25 to 175‰ by 1973 (Fig. 2). The ^{14}C maximum in subtropical surface ocean locations was delayed approximately ten years with respect to that in the atmosphere (see Fig. 1), illustrating the long residence time of $^{14}CO_2$ in the atmosphere (Druffel and Linick, 1978).

Sea surface temperature (SST) records reconstructed from $^{18}O/^{16}O$ ratios in coral bands (Druffel, 1985) are correlated with the $\Delta^{14}C$ records reported here in order to establish the relative controls that atmospheric exchange and surface circulation have on determining the ^{14}C content of equatorial waters. The effects of El Niño/Southern Oscillation (ENSO) events on SST (Druffel, 1985) and the ^{14}C cycle (Druffel, 1981) in the surface ocean have been shown to be significant in the tropical Pacific Ocean.

Reef-building corals incorporate DIC from sea water into their calcium carbonate

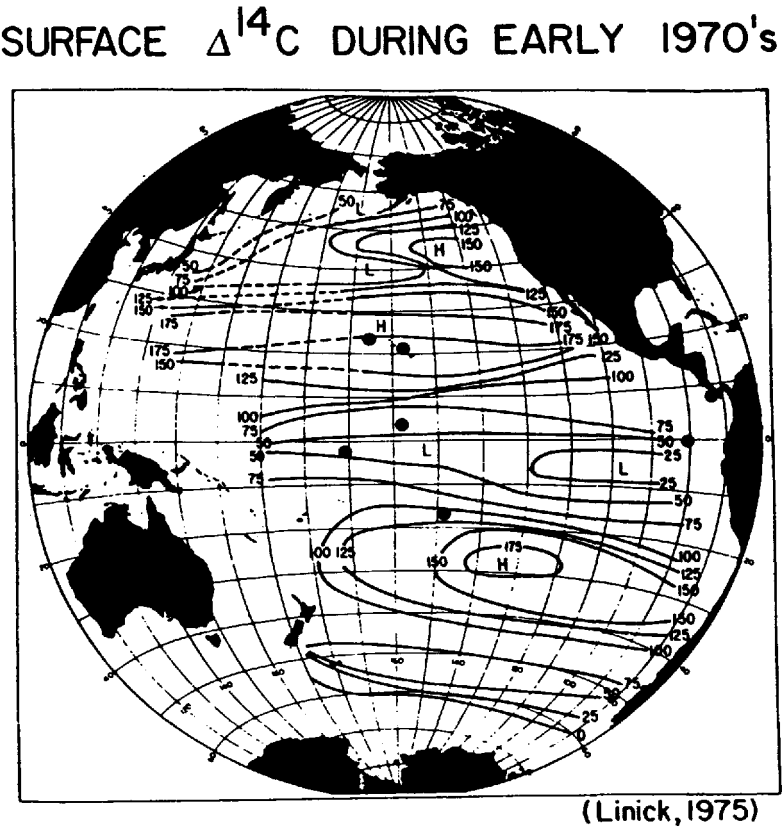

Figure 2. Isolines of bomb radiocarbon levels in surface waters of the Pacific Ocean during the early 1970's (after Linick, 1980). Sampling locations are indicated by (●).

(aragonite) skeletons. Weber and Woodhead (1972) showed that variation in the $^{18}O/^{16}O$ ratio ($\delta^{18}O$) in coralline aragonite is directly proportional to SST at the time of accretion, assuming constant salinity and water composition. Numerous authors have subsequently demonstrated a direct correlation between monthly averaged SST and $\delta^{18}O$ in subannual coral samples from the Atlantic and Pacific Oceans (Fairbanks and Dodge, 1979; Weil *et al.*, 1981; Dunbar and Wellington, 1981; Williams *et al.*, 1982; Druffel, 1985). Most hermatypic coral species studied to date contain annual variations in skeletal density which are discernible by x-ray of a thin slab (6–10 mm) cut along the axis of growth (Knutson *et al.*, 1972). As a result of the density band structure known periods of growth can be assigned to these coral bands, in the same manner that tree rings are dated. As aragonite does not dissolve in saturated surface waters, nor is it believed to exchange its carbonate with other sources of carbon, the accreted aragonite provides a permanent, unaltered record of the isotopic ratios present in sea water at the time of formation.

2. Sampling locations

Massive coral heads were collected from four sites in the tropical Pacific and three sites in the temperate Pacific (Fig. 2). Living *Porites* heads were gathered in July 1972 from the windward (east) side of Fanning Island (3°54'N, 159°12'W) near Rapa Pass (sample CFAN) (Chave and Kay, 1973) and in May 1979 from the leeward (west) side of Fanning Island near English Harbor (3°52'N, 159°23'W) (sample CTFN). *Porites* was also collected in September 1973 from a windward outer reef location of the NE coast of Canton Island (2°48'S, 171°43'W) (sample CCNT). Heads of *Pavona clavus* were collected from four sites in the Galapagos Islands (1S, 90W) (Santa Cruz, Hood and Duncan Islands and Urvina Bay). Results from all but one of these samples (Santa Cruz) were reported by Druffel (1981). The Urvina Bay sample (UB-16) stopped growing in 1953, during uplift of the shoreline due to volcanic activity (Richards, 1957). The other samples (SCI, HI, DI) were collected live from 1976 to 1982. *Porites* heads were obtained from two sites in the Hawaiian Islands: the SW shore of French Frigate Shoals (23°43'N, 166°06'W, sample CFFS) in November 1978 and Kahe Point on the SW shore of Oahu Island (COHU, 21°18'N, 158°07'W) in October 1978. A head of *Porites* was also collected from the NW coast of Tahiti (CMTH, 17°29'S, 149°36'W) in March 1974. A long series of *Gardinesoseris planulata* was collected live from Uva Island, Panama (CUVA, 7°48'N, 81°45'W) in July 1980.

All corals used for this project lived at depths of 10 m or less and were collected from outer reef locations that were flushed regularly with open ocean waters. The tropical study sites lie in the path of the South Equatorial Current, a westward flowing water mass that originates in the Peru Current (PC) along the western coast of South America. These waters are typically cool, nutrient-rich and depleted in oxygen (Reid, 1968; Eastropac Atlas; 1971, 1972, 1975). Equatorial upwelling, which is caused by the divergence of Ekman flow, is especially intense during the months of May through October when the southeast trade winds are strong.

3. Methods

The coral heads were collected using SCUBA, air dried and then cut with a rock saw along the vertical axes of corallite growth. Slabs were x-rayed to detect periodic variations in the density of the accreted aragonite. It was determined from $\delta^{18}O$ results that one of the Fanning corals (CFAN) and the Canton (CCNT) coral accreted two density band pairs per year, that is, two adjacent low and high density band couplets formed during a one year period (Druffel, 1985). The Tahitian coral appeared to accrete 5 bands per year. In contrast, the Hawaiian corals, CTFN (west Fanning), and the Galapagos corals (Druffel, 1981) accreted one band pair per year. The difference in density band periodicity most likely reflects the intensity of certain seasonally variant parameters (i.e. cloud cover, SST), and possibly mediated by reproductive cycles of the coral polyps (A. Szmant-Froelich, pers. comm.). X-radiographic analyses

revealed that CFAN grew from 1964–1972, CTFN from 1949–1979, CCNT from 1968–1973, UB-16 from 1929–1954, HI-6 (Hood) from 1960–1976, DI-12 (Duncan) from 1967–1977, CSCI from 1973–1982, CFFS from 1958–1978, COHU from 1970–1979, CMTH from 1969–1974, and CUVA from 1919–1980.

CSCI and CUVA were sectioned and analyzed at the Woods Hole Oceanographic Institution Radiocarbon Laboratory. CTFN was sectioned into annual bands at Lamont-Doherty by J. R. Toggweiler and analyzed for radiocarbon at the La Jolla Radiocarbon Laboratory. CFFS, COHU, and CMTH were sectioned and analyzed at La Jolla. Initially, CFAN and CCNT were sectioned into increments representing six months of growth and were analyzed for radiocarbon at La Jolla. The remainder of each of these coral heads was sectioned into growth increments representing several month intervals and analyzed for ^{14}C at WHOI. Approximately 1 month of growth per sample was removed due to the thickness of the saw blade. Stable isotope analyses were performed on monthly samples that were both drilled from the coral slabs (CFAN, CTFN, CCNT, HI-6) and averaged over an entire year (UB-16, HI-6). Results of the stable isotope analyses were reported by Druffel (1985).

Radiocarbon measurements were performed on coral samples that had been acidified and converted to acetylene via a lithium carbide intermediate. Four quartz gas proportional beta counters (volumes of 0.75, 1.5, 2.0 and 2.5 liters) were used to analyze the samples for radiocarbon. Each acetylene sample was counted for four to eight days at 900 mm of Hg and 21°C.

All radiocarbon measurements are reported in terms of $\Delta^{14}C$, which is the per mil (‰) deviation from the activity of nineteenth century wood (Stuiver and Polach, 1977):

$$\Delta^{14}C = \delta^{14}C - 2(\delta^{13}C + 25)(1 + \delta^{14}C/1000). \quad (1)$$

The results reported here have one sigma counting errors of ±3–4‰. Capability of ±2.0‰ precision was developed at the WHOI Radiocarbon Laboratory subsequent to the counting of these samples. All radiocarbon activity measurements were corrected for isotope fractionation to a $\delta^{13}C$ (relative to PDB-1) of −25.0‰ and for decay since the time of formation. The standard used was 95% of the net NBS oxalic acid count rate, corrected to a $\delta^{13}C$ of −19‰. Stable carbon and oxygen isotope ratios were measured on a V.G. Micromass 602E mass spectrometer.

4. Annual records of bomb radiocarbon

Time histories of post-bomb radiocarbon levels are reconstructed from analyses of annual coral bands from the temperate Pacific (Hawaiian Islands and Tahiti; Fig. 3b), and from the tropical Pacific Ocean (Fanning, Uva and Galapagos Islands; Fig. 3a and c). The $\Delta^{14}C$ results are listed in Tables 1 and 2.

Radiocarbon time-histories in the North Pacific rose from pre-bomb values of −50‰ in the early 1950's to a maximum value of 185‰ at the French Frigate Shoals

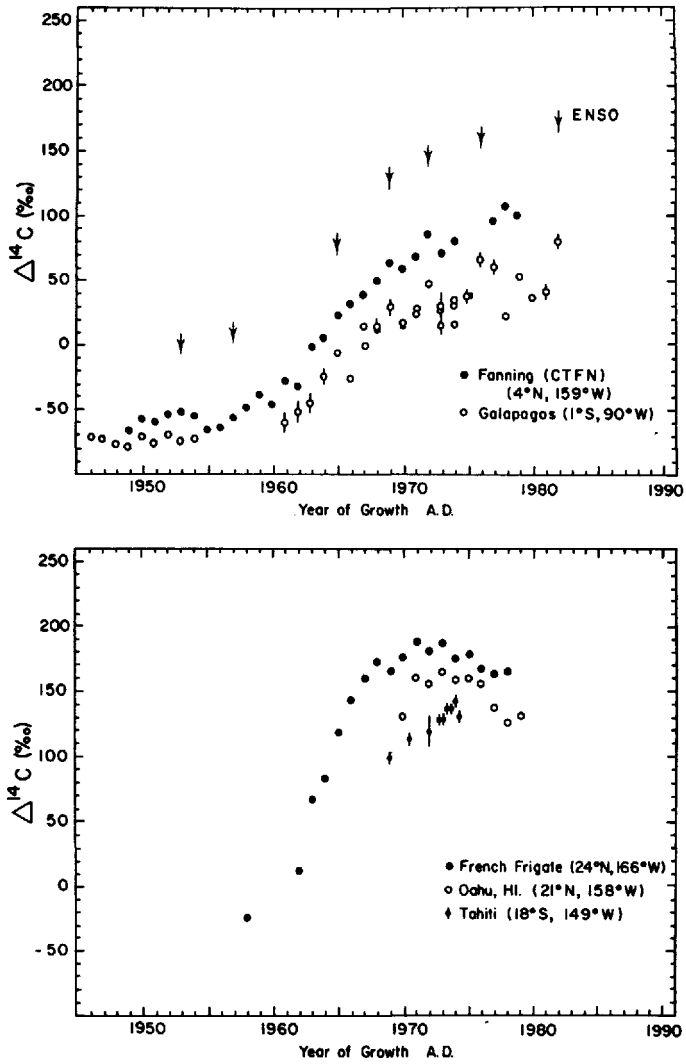

Figure 3. Time histories of radiocarbon in annual coral bands from (a) Fanning Island (CTFN, this work) and the Galapagos Islands (UB, HI, DI—Druffel, 1981; CSCI, this work); (b) French Frigate Shoals, Oahu and Tahiti; and (c) Uva Island (with French Frigate Shoals and Fanning results shown for comparison).

site by 1972 (Fig. 3b). Maximum values of only 165‰ were achieved at Oahu, a site farther away from the center of the mid-north Pacific gyre, and influenced more by North Equatorial Current waters. This agrees with GEOSECS data that show a gradient of surface $\Delta^{14}C$ from 145‰ at 17N (STN 235) to 187‰ at 31N (STN 213) during fall 1973.

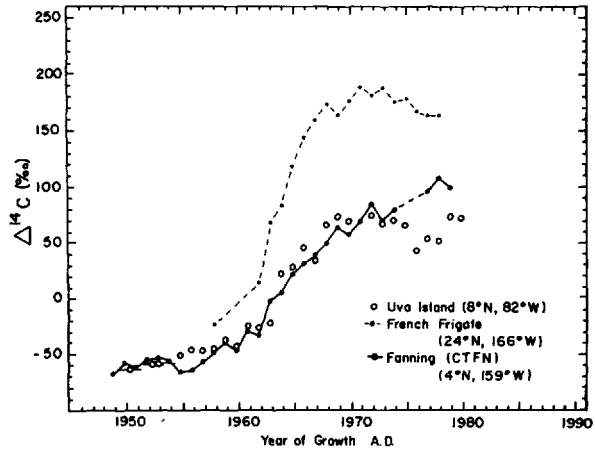

Figure 3. (Continued)

Table 1. Radiocarbon measurements of annual coral bands from Fanning (CTFN), Santa Cruz (CSCI), French Frigate Shoals (CFFS), Oahu, Hawaii (COHU), Tahiti (CMTH) and Uva Island, Panama (CUVA).

Sample no.	Known age	$\Delta^{14}C$ (‰)
Fanning Island (CTFN)		
LJ-5343	1949	−68
LJ-5342	1950	−58
LJ-5382	1951	−61
LJ-5417	1952	−55
LJ-5421	1953	−53
LJ-5366	1954	−56
LJ-5345	1955	−66
LJ-5385	1956	−64
LJ-5419	1957	−57
LJ-5344	1958	−49
LJ-5346	1959	−39
LJ-5371	1960	−47
LJ-5387	1961	−29
LJ-5383	1962	−33
LJ-5423	1963	−2
LJ-5422	1964	+6
LJ-5368	1965	22
LJ-5369	1966	32
LJ-5381	1967	39
LJ-5372	1968	50
LJ-5384	1969	64
LJ-5370	1970	58
LJ-5388	1971	69
LJ-5416	1972	85

Table 1. (Continued)

Sample no.	Known age	$\Delta^{14}C$ (‰)
LJ-5373	1973	71
LJ-5367	1974	80
LJ-5386	1977	96
LJ-5418	1978	108
LJ-5420	1979	100
Uva Island, Gulf of Chiriqui, Panama (CUVA)		
WH-42	1950–51	−64
WH-43	1952–53	−59
WH-68	1952–54	−58
WH-69	1955	−51
WH-70	1956	−46
WH-71	1957	−47
WH-72	1958	−45
WH-73	1959	−37
WH-74	1960	−42
WH-75	1961	−24
WH-115	1962	−26
WH-109	1963	−22
WH-110	1964	23
WH-106	1965	29
WH-112	1966	46
WH-108	1967	34
WH-111	1968	66
WH-113	1969	74
WH-114	1970	70
WH-96	1972	75
WH-94	1973	67
WH-99	1974	70
WH-92	1975	56
WH-95	1976	43
WH-93	1977	54
WH-91	1978	52
WH-97	1979	74
WH-98	1980	73
Santa Cruz Island, Galapagos (CSCI)		
WH-162	1973	28
WH-140	1974	36
WH-147	1975	39
WH-136	1976	68
WH-135	1977	63
WH-133	1978	24
WH-132	1979	54
WH-134	1980	38

Table 1. (Continued)

Sample no.	Known age	$\Delta^{14}C$ (‰)
WH-142	1981	46
WH-137	1982	80
French Frigate Shoals (CFFS)		
LJ-4941	1958	23
LJ-4940	1962	14
LJ-4948	1963	68
LJ-4942	1964	84
LJ-4947	1965	118
LJ-4943	1966	144
LJ-4945	1967	159
LJ-4946	1968	173
LJ-4944	1969	164
LJ-4933	1970	177
LJ-4939	1971	189
LJ-4937	1972	182
LJ-4934	1973	188
LJ-4938	1974	177
LJ-4931	1975	179
LJ-4935	1976	168
LJ-4932	1977	164
LJ-4936	1978	165
Oahu, Hawaii (COHU)		
LJ-5329	1970	131
LJ-5328	1971	161
LJ-5327	1972	156
LJ-5326	1973	166
LJ-5323	1974	159
LJ-5324	1975	161
LJ-5325	1976	157
LJ-5322	1977	139
LJ-5321	1978	127
LJ-5320	1979	132
Tahiti (CMTH)		
LJ-5229	1969	99
LJ-5227	1970.5	113
LJ-5224	1972	118
LJ-5222	1972.6	128
LJ-5221	1973	128
LJ-5220	1973.3	136
LJ-5219	1973.6	136
LJ-5218	1974	142
LJ-5217	1974.2	130

Table 2. Radiocarbon measurements of subannual coral bands from Fanning (CFAN) and Canton Islands.

Sample no.	Growth period	Number of months	$\Delta^{14}C$ (‰)
Fanning Island			
LJ-5127	July–Dec. 1964	6	21
LJ-5126	Jan.–June 1965	6	37
LJ-5125	July–Dec. 1965	6	44
LJ-5123	Jan.–June 1966	6	54
LJ-5124	July–Dec. 1966	6	64
LJ-5121	Jan.–June 1967	6	49
LJ-5120	July–Dec. 1967	6	66
LJ-5122	Jan.–June 1968	6	61
LJ-5106	July–Dec. 1968	6	68
LJ-5105	Jan.–June 1969	6	64
LJ-5104	July–Dec. 1969	6	73
LJ-5102	Jan.–June 1970	6	69
LJ-5103	June–Dec. 1970	7	69
LJ-5100	Jan.–Mar. 1971	3	56
LJ-5101	Apr.–July 1971	4	74
LJ-5043	Aug. 1971–Mar. 1972	9	97
LJ-5042	Apr.–June 1972	3	84
WH-55	May–June 1970	1	89
WH-54	Aug.–Nov. 1970	3	72
WH-52	Dec.–Mar. 1971	3	71
WH-53	Apr.–July 1971	3	84
WH-48	Aug.–Oct. 1971	2	83
WH-49	Nov.–Mar. 1972	4	101
WH-46	Apr.–July 1972	3	104
Canton Island (CCNT)			
LJ-5063	Mar.–Aug. 1968	6	40
LJ-5062	Sept.–Feb. 1969	6	59
LJ-5058	Mar.–Aug. 1969	6	48
LJ-5057	Sept.–Feb. 1970	6	56
LJ-5064 dup.	Mar.–Aug. 1970	6	58
LJ-5050	Mar.–Aug. 1970	6	60
LJ-5065 dup.	Sept.–Feb. 1971	6	49
LJ-5049	Sept.–Feb. 1971	6	65
LJ-5048	Mar.–Oct. 1971	8	66
LJ-5056 dup.	Nov. 1971–Oct. 1972	12	73
LJ-5046 dup.	Nov.–Oct. 1972	12	68
LJ-5044	Nov.–Oct. 1972	12	69
LJ-5045	Nov.–May 1973	7	80
LJ-4984 dup.	June–Sept. 1973	3	74
LJ-5047	June–Sept. 1973	3	80
WH-61	Mar.–June 1971	3	90

Table 2. (Continued)

Sample no.	Growth period	Number of months	$\Delta^{14}C$ (‰)
WH-59	July–Oct. 1971	3	57
WH-56	Nov. 1971–Mar. 1972	4	73
WH-60	Apr.–Oct. 1972	6	78
WH-58	Nov. 1972–Feb. 1973	3	84
WH-57	Mar.–May 1973	2	79
WH-63	June–July 1973	2	76
WH-62	Aug.–Sept. 1973	2	92

In the South Pacific, limited data (Table 1, Fig. 3b) show a steady increase in $\Delta^{14}C$ from 100‰ in 1969 to about 140‰ by 1974. These results agree with GEOSECS seawater measurements of spring 1974 that range from 141‰ (STN 317) to 155‰ (STN 324) in the upper 50 m (Ostlund and Stuiver, 1980). Sea water $\Delta^{14}C$ has subsequently decreased in the South Pacific to about 125‰ by 1979 (Quay *et al.*, 1983). In general, bomb radiocarbon in the southern hemisphere (Tahiti) is lower than that at similar latitudes in the northern hemisphere (Oahu) and appears to still be rising in the mid-1970's while the northern values had reached a plateau. This is because all of the bomb radiocarbon was introduced to the northern hemisphere from the stratosphere and subsequently transported to the south via tropospheric mixing processes (mixing time 1–2 years). Figure 1 illustrates the lag in atmospheric bomb radiocarbon maxima between the northern and southern hemisphere during the mid-1960's.

At the mid-tropical Pacific site (CTFN), $\Delta^{14}C$ values rose from −65‰ in the early 1950's to 105‰ by 1979 (Fig. 3a). Previously published values from the Galapagos (UB-16, Druffel, 1981) averaged −75‰ during the early 1950's. Analyses obtained from Santa Cruz Is. coral reveal $\Delta^{14}C$ values of 50–60‰ by 1982. Higher $\Delta^{14}C$ values appear during ENSO years (1965, 1969, 1972–73, 1976, 1982–83) at the Fanning and Galapagos sites (Fig. 3a). This is caused by increased retention of bomb radiocarbon in the surface waters due to a reduction of Ekman divergence at the equator. In addition, the reduction in the pCO_2 gradient between air and sea that has been observed during ENSO causes an increase in the net flux of radiocarbon from air to sea.

Overall, $\Delta^{14}C$ values are lower at the Galapagos Islands because of increased upwelling in the eastern equatorial Pacific. The Peru Current, which supplies most of the water to this area, is heavily influenced by coastal upwelling which takes place along the coast of South America. Ekman divergence at the equator also contributes to the low $\Delta^{14}C$ values in the Galapagos corals.

A noticeable increase in $\Delta^{14}C$ appears in the Fanning Island record during the early 1950's. A rise of about 10–15‰ is apparent by 1952. Values remained high until 1954 and then dropped to baseline values (−65‰) by 1955. The amount of ^{14}C produced

as a result of ground level nuclear weapons testing in the Marshall Islands between 1952 and 1954 was about 6.5% of the total bomb-^{14}C produced (950×10^{26} atoms) (Federal Radiation Council, 1963). As a result of these blasts, radiocarbon concentration rose in the atmosphere and was recorded in northern hemisphere tree rings by 1953 (Cain and Suess, 1976) and by 1955 $\Delta^{14}C$ had risen substantially (to +30‰). Considering the large impedence for CO_2 exchange at the air-sea interface, we would not expect to notice a rise in radiocarbon in average surface waters in the world ocean until 1957 or so. The presence of bomb radiocarbon in the Fanning coral during 1952–1954 suggests that the area was exposed to close-in fallout of bomb-produced radiocarbon either in particulate form (i.e. adsorbed onto CaO particles produced during the vaporization of coral reefs by the bombs) or in the gas phase. Using a box diffusion model to calculate exchange of isotopic carbon between air and sea (Emanuel *et al.*, 1984), $\Delta^{14}C$ of atmospheric CO_2 would have been 60–100‰ for two years (or 280‰ for one year) in order to raise the $\Delta^{14}C$ of tropical sea water from −65‰ to −50‰. A prolonged local rise in atmospheric radiocarbon levels for more than a few months could only have been achieved if there was a constant source of bomb radiocarbon from numerous tests over a two year period, which was indeed the case (Federal Radiation Council, 1963). Presence of bomb fallout during this period is confirmed by the distribution of ^{90}Sr reported by Toggweiler and Trumbore (1985) for the same Fanning coral head used in this study. ^{90}Sr was detected in all of the growth bands analyzed, the oldest being 1952. It is not possible to determine, however, whether the early peak in bomb radiocarbon can be attributed to either fallout or isotopic exchange with the atmosphere.

Figure 3c shows the radiocarbon measurements from Uva Island (8N, 82W), with the data from Fanning Island and French Frigate Shoals shown for comparison. Pre-bomb and post-bomb $\Delta^{14}C$ values up to about 1963 at Uva are very similar to those found at Fanning Island. There is evidence of bomb ^{14}C from the early ground tests of the 1950's in the Uva data, however the peak appears 2–3 years delayed from that in the Fanning Island data. $\Delta^{14}C$ values were higher at Uva than they were at Fanning during the late 1960's, but not as high as those at French Frigate Shoals in the northern gyre. This trend is a function of Uva's intermediate position between the equatorial upwelling zone and mid-gyre locations. This region appears to be influenced by both the ^{14}C-rich North Equatorial Countercurrent (Konishi *et al.*, 1981) and the moderate upwelling (^{14}C-poor) that predominates the Panama Basin region.

An unexpected decline in $\Delta^{14}C$ of about 30‰ occurs at Uva from 1974 to 1976. Stable oxygen isotope ratios ($\delta^{18}O$) performed on the same annual coral bands (Druffel *et al.*, in prep.) reveal a steady increase of 0.55‰ from 1970 to 1977. If this change is attributed purely to changes in annually-averaged SST, and not to changes in salinity and water composition, then a cooling of 2–3°C is suggested. $\delta^{13}C$ values, which have been shown to be indicators of water mass in some corals (Nozaki *et al.*, 1978) decreased dramatically (by 0.65‰) during a slightly later time period (1974–1979). It

appears that the mid-1970's was marked by a significant increase in upwelling in the Panama region. There does not appear to be a rise in $\Delta^{14}C$ associated with ENSO events at Uva Island.

The tropical ^{14}C records (Fig. 3a) are different from the temperate ^{14}C records (Fig. 3b) in two respects: (1) the maximum $\Delta^{14}C$ values achieved in the Pacific gyre regions (145–185‰) were far greater than those at the tropical sites (50–105‰), and (2) maximum $\Delta^{14}C$ values were not reached in the tropical Pacific in the early 1970's, and they appear not to have been reached even by as late as 1982.

The slope of pre-1970 $\Delta^{14}C$ values at a given location appears proportional to the residence time of water at the surface. Influenced predominantly by downwelling, North Pacific gyre waters stay at the surface for much longer periods, in contrast to tropical surface waters where upwelling of ^{14}C depleted waters is the predominant mixing process. Thus, subtropical gyre waters accrue bomb ^{14}C from the atmosphere at a faster rate, causing the levels to rise much quicker than at tropical surface locations. $\Delta^{14}C$ values in temperate regions decrease dramatically after 1975, whereas those in tropical locations were still rising by the early 1980's. This is caused by the downward diffusion and horizontal advection of bomb-enriched temperate waters along submerged isopycnals, subsequent transport via major circulation pathways to lower latitudes, and upwelling to the surface at the equator. Quay *et al.* (1983) found evidence by 1979 of well-defined subsurface tongues of high ^{14}C, both north and south of the equator in the Pacific. Horizontal transport of high-^{14}C temperate waters toward lower latitudes cause ^{14}C levels at the equator to continue to rise, and result in an overall relative depletion of the ^{14}C inventory at higher latitudes. Eventually, radiocarbon at temperate and tropical surface locations will approach a common $\Delta^{14}C$ value. Extrapolating the trends from 1970 in Figures 3a and b, it appears that this may occur in the mid-1980's, although present data sets are insufficient to corroborate this. Despite the surface $\Delta^{14}C$ trends, bomb radiocarbon water column inventories in temperate regions of the world ocean are still significantly higher than those initially delivered from the atmosphere (Broecker *et al.*, 1985), due to the deeper penetration of the bomb radiocarbon transient at these latitudes.

5. Seasonal records of bomb radiocarbon

Post-bomb radiocarbon measurements of semi-annual growth bands from the mid-Pacific corals (open circles) are presented in Figure 4a and b. Levels were 10–20‰ lower at Canton than at Fanning, most likely due to Canton's proximity to the equator (by 1.5° of latitude) and thus, a stronger influence from equatorial upwelling.

Radiocarbon levels during the major 1972 ENSO appear higher than that during surrounding years. This anomaly is greater at the Fanning location, most likely a result of the fact that the ENSO phenomenon is more prominent toward the eastern equatorial Pacific. There appears to be only slightly higher $\Delta^{14}C$ values (by $\leq$15‰) at the two sites associated with the moderate ENSO event of 1969.

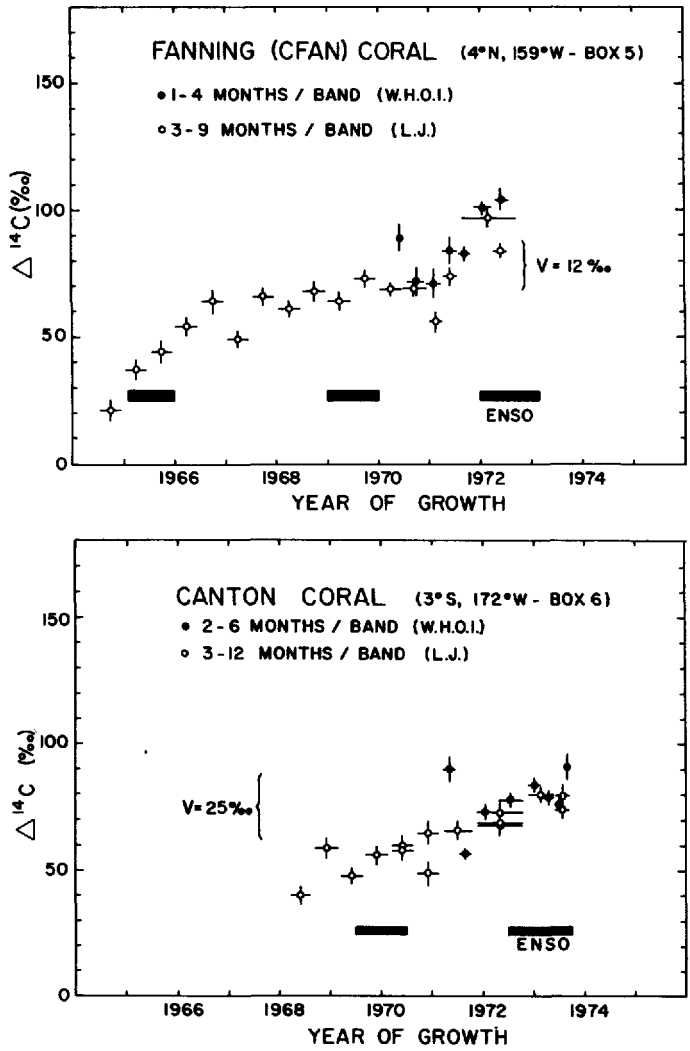

Figure 4. (a) $\Delta^{14}C$ measurements of seasonal (●) and 6 month (○) intervals from Fanning Island (4N, 159W) coral. (b) $\Delta^{14}C$ measurements of seasonal (●) and six-month (○) intervals from Canton Island (3S, 172W) coral.

Superimposed on these major trends is an annual oscillation with an amplitude of 4–5‰. Higher $\Delta^{14}C$ values are present during the middle of the year. However, conclusions regarding the seasonal nature of ^{14}C cannot be drawn from these data, as the 6-month sampling interval has caused attenuation and most likely a large shift of the actual peaks and valleys in the seasonal ^{14}C record.

There is a slight disparity between the CFAN and CTFN results (both Fanning Is.),

in that $\Delta^{14}C$ from CFAN (see Fig. 4a) was about 10‰ higher than that from CTFN during 1966–1968. It seems unlikely that $\Delta^{14}C$ values from two open ocean regions on opposing sides of the same island (18 km diameter) could vary by this much. Improper assignment of band years is not likely for the CTFN coral as stable isotope ratios measured on a subannual basis (see Druffel, 1985) revealed a good correlation between unusually low $\delta^{18}O$ values and ENSO events between 1953 and 1976. However, as stable isotope measurements were not run for the early period in the CFAN coral, it is possible that the age assignments of these early bands are ±1 year.

The $\Delta^{14}C$ values measured in several month samples from the Fanning and Canton corals (filled circles) also appear in Figure 4a and b. The seasonal variation of $\Delta^{14}C$ at Fanning during the non-El Niño period of 1970–71 appears to have been about 12‰. Levels were low (72‰) during the beginning of 1971 and higher (84‰) during the northern summers of 1970 and 1971. At first, these data appear to be inconsistent with major upwelling patterns in the tropical Pacific, as the southeast tradewinds which drive the Peru and South Equatorial Current systems (sources of low ^{14}C water) are strongest during mid-year. However, due to weak northeasterly winds, northward transequatorial Ekman transport of upwelled waters is at a minimum during mid-year (Wyrtki, 1981). The result of these opposing factors apparently yields high $\Delta^{14}C$ during northern summer.

Very high $\Delta^{14}C$ values (up to +101–104‰) were achieved during the early part of the major 1972–73 ENSO. During the early 1970's, values this high were recorded in the Pacific at locations north of 10N (Linick, 1978; Ostlund and Stuiver, 1980; see Fig. 2). This is not to imply that water from 10–15N traversed to the equator. More likely, the South Equatorial Current flow had virtually ceased and upwelling was so severely hampered that nearly all of the bomb $^{14}CO_2$ that entered the surface ocean from the atmosphere was retained in the upper 50 m or so of the water column, with very little being advected away from the equatorial zone due to reduced Ekman divergence. This would cause a dramatic increase in ^{14}C over a short period of time, as there was still a large gradient in $\Delta^{14}C$ between the atmosphere (500‰) and equatorial surface ocean (80‰) in the early 1970's. This dramatic rise in ^{14}C was accompanied by a reduction in $\delta^{18}O$ of .2–.4‰ (Fig. 5), which is indicative of a 1–2°C rise in SST (assuming a correlation of .22‰ per 1°C [Fairbanks and Dodge, 1979]).

Radiocarbon measurements of banded corals from Canton Island show good agreement for 3 of the 4 duplicate analyses performed on separate samples of the same band cut from different sections of the coral head (see Table 2). Also, for the June–September 1973 growth interval, agreement within 2 sigma counting error was obtained for averages of $\Delta^{14}C$ measurements from the La Jolla (LJ-5047 and 4984; 77 ± 3‰) and Woods Hole (WH-62 and 63; 82 ± 3‰) laboratories.

The $\Delta^{14}C$ trend obtained from the seasonal Canton samples is quite different from that obtained for Fanning. A seasonal signal with a variation of about 25‰ seems apparent during the period 1971–72. This appears twice as large as the seasonal signal

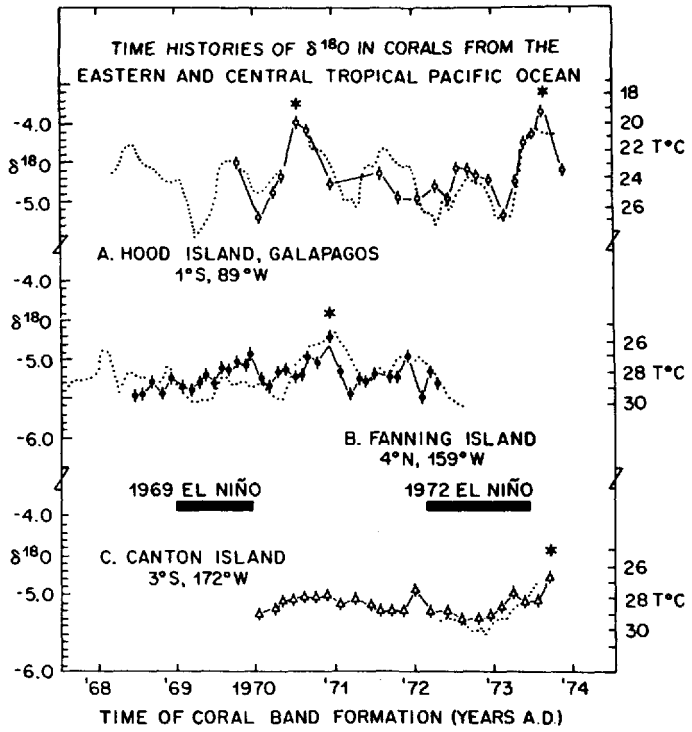

Figure 5. Time histories of $\delta^{18}O$ in subannual samples of coral from the east and mid-Pacific Ocean during the period 1968–1974. Sea surface temperature (SST) for each location is shown by the dotted lines. The SST record plotted for Fanning is from Christmas Island (2N, 157W) (after Druffel, 1985).

observed in the Fanning Island coral. It is also apparent that the seasonal signal at Canton is several months out of phase from that at Fanning. South of the equator, transequatorial Ekman transport is greatest during mid-year which, when coupled with the maximum South Equatorial Current flow, is responsible for very low $\Delta^{14}C$ values during the southern winter.

At first glance, there appears to be no rise in $\Delta^{14}C$ above normal levels (84‰) at Canton during the major ENSO of 1972–73. However, closer scrutiny reveals that the reduction of $\Delta^{14}C$ was only 10–15‰ during mid-1973, not as pronounced as the seasonal variation (~25‰) observed during 1971–72. It is difficult to determine the seasonal variation during 1972, due to the very large sampling interval for the late-72 sample. Nonetheless, $\Delta^{14}C$ values appear high during 1973, most likely due to reduced Ekman divergence and higher net input of $^{14}CO_2$ to the surface ocean during the 1972–73 ENSO. The retention of high $\Delta^{14}C$ values at the Canton site occurred 6–12 months later than the appearance of high values at the Fanning site (Fig. 6) during the

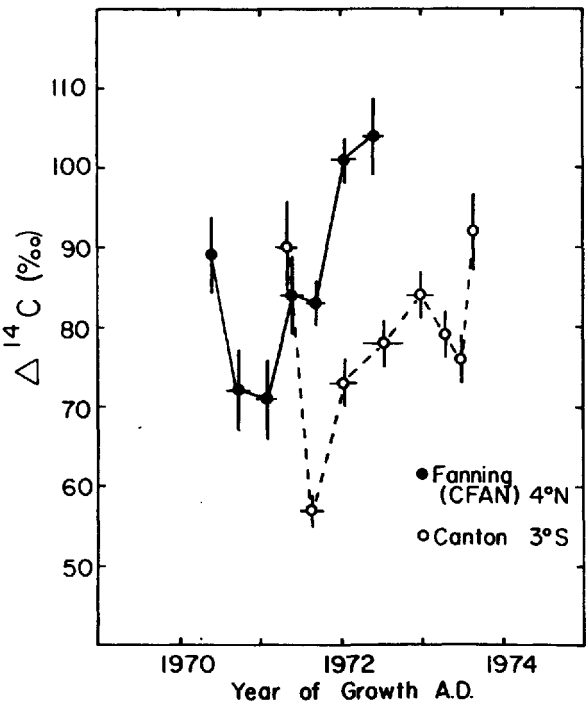

Figure 6. Seasonal radiocarbon trends at Fanning (●) and Canton (○) Islands. The radiocarbon minima at these locations were offset by three to six months.

'72–'73 ENSO. This is in agreement with Wyrtki's (1975a) observation that ENSO occurs later at locations south of the equator in the mid-Pacific.

It is noteworthy that $\delta^{18}O$ values at Canton decreased 0.1–0.2‰ (Fig. 5) during late 1972 which represents a 0.5–1°C increase in SST. The rise in $\Delta^{14}C$ per °C warming during this period was similar at both the Fanning ($25/1.5 = 15‰\ °C^{-1}$) and Canton ($13/0.8 = 16‰\ °C^{-1}$) sites. In addition, $\Delta^{14}C$ rose 25‰ above normal levels during the 1972 ENSO in the Galapagos Islands (Druffel, 1981), and was accompanied by a rise in $\delta^{18}O$ of 0.6‰ ($24/2.5 = 10‰\ °C^{-1}$). These results are consonant with observations by Burling and Garner (1959) and Nydal and Loveseth (1983) of a direct correlation between SST and $\Delta^{14}C$ in the Atlantic and Pacific Oceans. This correlation suggests that similar processes affect the surface waters in the equatorial Pacific during ENSO, that is, waters of similar origin invade or are retained for extended periods of time at each site.

It also may be possible that the rise in $\Delta^{14}C$ during the '72–'73 ENSO was the result of higher latitude, high ^{14}C water just beginning to arrive in the equatorial region. However, even as late as December 1973 GEOSECS $\Delta^{14}C$ profiles in the western Pacific showed no evidence of subsurface tongues of high ^{14}C north or south of the

equator (Ostlund and Stuiver, 1980), which supports retention of atmospheric $^{14}CO_2$ as the cause of high $\Delta^{14}C$ during ENSO.

6. Discussion

Certain characteristics of the $\Delta^{14}C$ records in corals provide valuable information for understanding near surface circulation and the chemical cycling of carbon in the tropical Pacific Ocean. First, the banded coral records clearly show that ^{14}C levels near the equator were initially much lower than at subtropical locations in the 1960's and early 1970's due to upwelling, but later rose due to input of horizontally-advected, bomb-laden waters from higher latitudes. Second, a larger seasonal ^{14}C signal was found at 3S than at 4N, which appears to reflect substantial differences in circulation patterns between the two areas. Third, elevated levels of ^{14}C and SST at both tropical locations (3S and 4N) during the 1972–73 ENSO is suggestive of widespread changes in the cycling of $^{14}CO_2$ during periods of significant climate change. Fourth, the similarity of the post-1975 $\Delta^{14}C$ records from the mid- and eastern equatorial sites is suggestive of the importance of the South Equatorial Current flow to the mid-tropical Pacific. It is shown in the following discussion that the South Equatorial Current flow varies in magnitude seasonally in order to explain the seasonal variations of $\Delta^{14}C$ observed at the Fanning and Canton sites.

Quay *et al.* (1983) reported an estimate of the upwelling transport rate in the equatorial Pacific using a multi-layer mixing model applied to ^{14}C and various chemical parameters measured in April 1979 on the NORPAX FGGE shuttle. Their calculations were based on the assumption that meridional advection resulting from geostrophic flow is the main source of water to the surface equatorial zone. They assumed that continued increase in ^{14}C levels after 1970 in the central equatorial Pacific, while ^{14}C levels in the eastern equatorial Pacific remained constant, cannot be the result of westward transport of surface water. It is shown here, however, that ^{14}C levels in the eastern equatorial Pacific were *not* constant after 1970. Radiocarbon measurements of corals from Santa Cruz Island in the eastern tropical Pacific (Fig. 3a) show a rise of about 25‰ from 1970–1982, compared to a rise of 50‰ in the central tropical Pacific (Fanning Island). In light of this evidence, and the unexpectedly large seasonal variations of $\Delta^{14}C$ in the central tropical Pacific (12–25‰), it is apparent that the South Equatorial Current, which originates in the eastern equatorial Pacific, is a nontrivial source of water to the central equatorial Pacific.

Wyrtki (1981) determined from wind stress data that the Ekman divergence in the central equatorial Pacific is 84×10^6 m^{3}s^{-1}. Wyrtki and Kilonsky (1984) estimated an annually averaged South Equatorial Current contribution to this latitude range (0–50 m depth) on the order of 12×10^6 m^{3}s^{-1}. Using direct current measurements, Firing (1981) estimated that the South Equatorial Current flow was 20×10^6 m^{3}s^{-1} between 3N and 3S (150–158W). It appears that there is overwhelming evidence for a

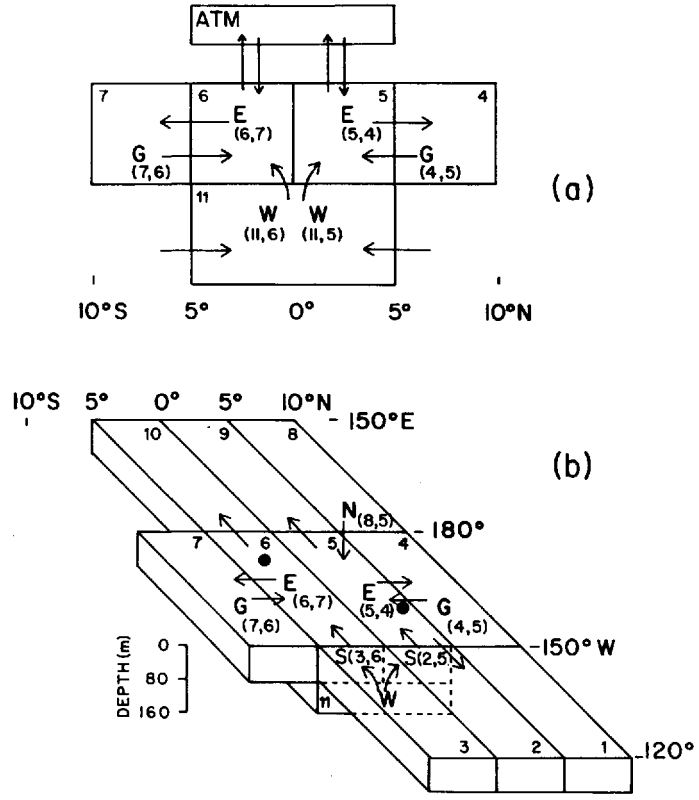

Figure 7. Schematic representation of three-dimensional advective box model used to quantify the seasonal contribution of water and radiocarbon to the two mid-tropical Pacific sites (●). (a) Meridional flow of water and ^{14}C; (b) Meridional and zonal flow of water and ^{14}C.

substantial input of South Equatorial Current water to the central equatorial Pacific. Estimates of the zonal South Equatorial Current flow on both an annual and a seasonal basis will be made using a simple advective box model.

a. Annual model. A time-stepped, advective, multi-box model calculation is used to calculate ^{14}C concentrations in the equatorial boxes north (Fanning, box 5) and south (Canton, box 6) of the equator. The purpose of this modelling exercise is to determine the importance of the South Equatorial Current for the time history of bomb radiocarbon in the central equatorial Pacific. A schematic portrayal of the box model is shown in Figure 7. The equatorial ocean is divided into four latitude bands (10-5S, 5S-0, 0-5N and 5-10N) and three longitude bands (150E-180, 180-150W and 150-120W).

The net flux of radiocarbon into boxes 5 and 6 is equal to the fluxes into minus the fluxes out of each box:

$$\begin{aligned}\Delta\Sigma^{14}CO_2\,(5)_{t+\Delta t} = [&G(4,5)_t\,\Sigma^{14}CO_2(4)_t + W(11,5)_t\,\Sigma^{14}CO_2(11)_t \\ &+ S(2,5)_t\,\Sigma^{14}CO_2\,(2)_t + N(8,5)_t\,\Sigma^{14}CO_2(8)_t \\ &+ I(A)_t F_t - [E(5,4)_t + S(5,9)_t \\ &+ N(5,2)_t]\,\Sigma^{14}CO_2(5)_t - I(5)_t] \cdot [G(4,5)_t \\ &+ W(11,5)_t + S(2,5)_t + N_5(8,5)_t]^{-1} \end{aligned} \tag{2}$$

$$\begin{aligned}\Delta\Sigma^{14}CO_2\,(6)_{t+\Delta t} = [&G(7,6)_t\,\Sigma^{14}CO_2(7)_t + W(11,6)_t\,\Sigma^{14}CO_2(11)_t \\ &+ S(3,6)_t\,\Sigma^{14}CO_2(3)_t + I(A)_t F_t - [E(6,7)_t \\ &+ S(6,10)_t]\,\Sigma^{14}CO_2(6)_t - I(6)_t] \cdot [G(7,6)_t \\ &+ W(11,6)_t + S(3,6)_t]^{-1} \end{aligned} \tag{3}$$

where $\Delta\Sigma^{14}CO_2\,(i)_{t+\Delta t}$ is the total increase of $DI^{14}C$ concentration (moles m^{-3}) in box i during Δt, $\Sigma^{14}CO_2(i)$ is $\Sigma^{14}CO_2$ concentration (moles m^{-3}) in box i, $G(i,j)$ is the geostrophic flow ($\times 10^6$ m^3s^{-1}) from box i to box j, $W(i,j)$ is the upwelling flux ($\times 10^6$ m^3s^{-1}) from box i to box j, $S(i,j)$ is the flux ($\times 10^6$ m^3s^{-1}) of South Equatorial Current water from box i to box j, $N(i,j)$ is the flux ($\times 10^6$ m^3s^{-1}) of North Equatorial Counter Current water from box i to box j, $E(i,j)$ is the Ekman divergence ($\times 10^6$ m^3s^{-1}) from box i to box j [where $E(i,j) = G(j,i) + W(11,i)$], and $I(i)$ is the invasion rate of $^{14}CO_2$ (moles) across the air/sea (box i) interface during interval Δt. F is the factor controlling $^{14}CO_2$ input to the ocean and is <1 due to the high pCO_2 in the equatorial waters (pCO_{2s}) as compared to atmospheric values (pCO_{2a}) (Broecker & Peng, 1983), where:

$$F_t = \frac{(\Delta^{14}C_a/.983 - \Delta^{14}C_s \cdot (pCO_{2s}/pCO_{2a}))}{(\Delta^{14}C_a/.983 - \Delta^{14}C_s)} \tag{4}$$

It is assumed that each box is well mixed and contains a homogenous $\Delta^{14}C$ value at time t. The depth of the mixed layer and that of the subsurface layer were assigned on the basis of bomb radiocarbon and tritium distributions observed in the upper water column during GEOSECS (Fig. 8a and b). $\Delta^{14}C$ values were relatively constant from the surface to depths of about 160 m. Tritium displayed similar behavior, except at the equator. Based on these distributions, the bottom of the mixed layer is assigned as 80 m and that of the subsurface layer is 160 m. The base of the subsurface layer (160 m) is similar to estimates of the maximum depth of upwelling in the equatorial Pacific, which are 135 m (Fine *et al.*, 1987), 180 m (Bryden and Brady, 1985) and 225 m (Quay *et al.*, 1983). It is important to note that the GEOSECS data, which were taken two years subsequent to our observed seasonal variations in corals, still show that upwelling waters contained lower levels of bomb radiocarbon and were thus a source of ^{14}C-depleted waters to boxes 5 and 6 from 1971–1973.

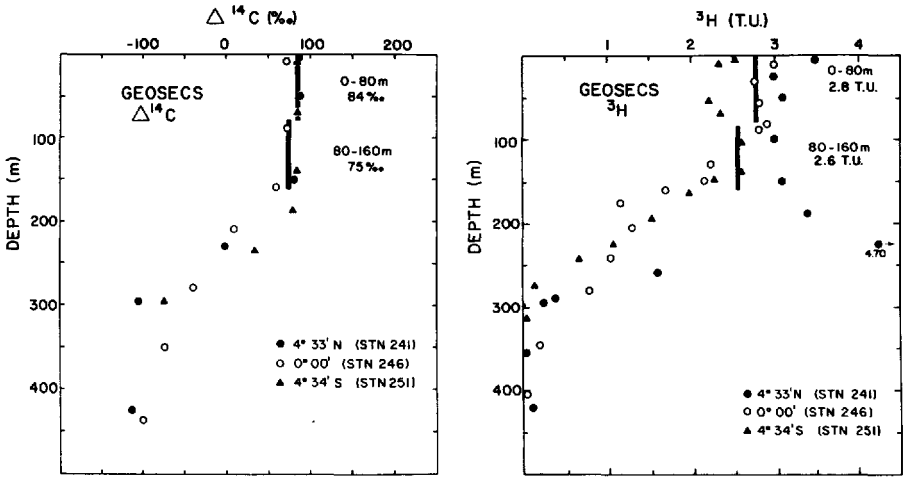

Figure 8. (a) $\Delta^{14}C$ in the upper 500 m of the equatorial Pacific during December 1973 (Ostlund and Stuiver, 1980). (b) Tritium in the upper 500 m of the equatorial Pacific during December 1973 (Ostlund *et al.*, 1979).

Estimates of Ekman flow are obtained from Wyrtki (1981) and scaled according to the smaller boxes used here (annually-averaged $E(6, 7) = 14.7 \times 10^6$ m^{3}s^{-1} and $E(5, 4) = 13.3 \times 10^6$ m^{3}s^{-1}). This is compensated by geostrophic convergence of the same magnitude as determined from the east-west pressure gradient (Wyrtki, 1981), only a portion of which is transported above the base of the mixed layer ($G(7, 6) = 8.0 \times 10^6$ m^{3}s^{-1}, $G(4, 5) = 6.0 \times 10^6$ m^{3}s^{-1}). The remainder of the geostrophic convergence (below 80 m), plus the decrease in the transport of the equatorial Undercurrent is upwelled from box 11 into boxes 5 and 6 ($W(11, 6) + W(11, 5) = 14.5 \times 10^6$ m^{3}s^{-1}). A total value of 7×10^6 m^{3}s^{-1} is chosen to represent the South Equatorial Current flow into the mixed layer of the central Pacific based on studies of the FGGE data by Wyrtki and Kilonski (1984), where annually-averaged flows of $S(2, 5) = 3 \times 10^6$ m^{3}s^{-1} and $S(3, 6) = 4 \times 10^6$ m^{3}s^{-1}. The North Equatorial Counter Current, $N(8, 5)$, constitutes a significant flow (2×10^6 m^{3}s^{-1}) into box 5 during October–March, when it is at its southernmost extent (Wyrtki, 1975).

The flushing time of boxes 5 and 6 is very short, which is justification for ignoring diffusion as a mixing process in the model. If the volume of the surface layer [80 m deep, 30° long and 10° wide] is 3.0×10^{14} m^3, and the flow of water from the various sources into boxes 5 and 6 is 35.5×10^6 m^{3}s^{-1}, then the residence time of water in our two surface boxes is 3.2 months.

Bomb radiocarbon time histories in the flows $G(4, 5)$, $G(7, 6)$, $W(11, i)$, $S(2, 5)$, $S(3, 6)$ and $N(8, 5)$ are shown in Figure 9a to f. Measurements of sea water DIC (Bien and Suess, 1967; Linick, 1978; Ostlund and Stuiver, 1980; Quay *et al.*, 1983) and of banded corals (Druffel, 1981; Konishi *et al.*, 1981; this work) were used to construct

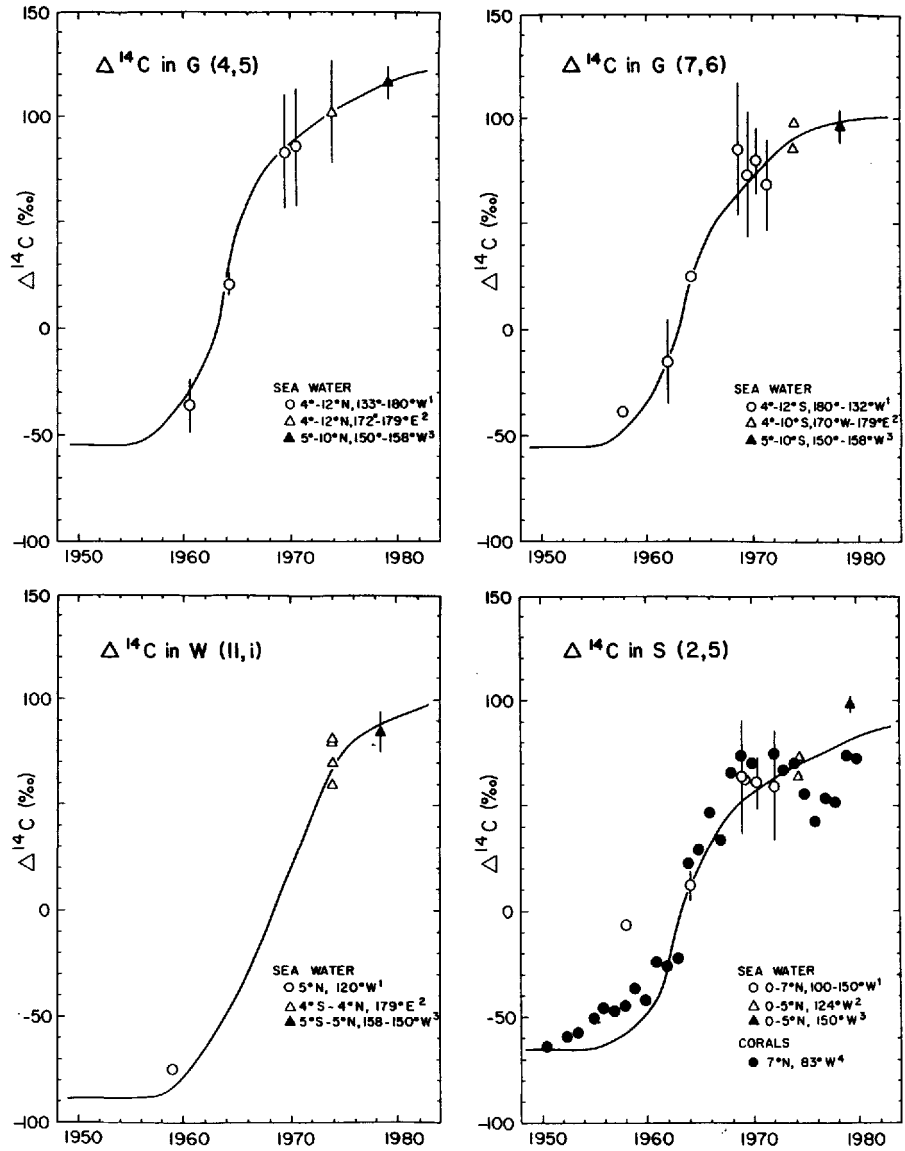

Figure 9a-f. Time histories of bomb $\Delta^{14}C$ in the various currents and water masses involved in the annual model. [1—Linick, (1978); 2—Ostlund and Stuiver (1980); 3—Quay *et al.* (1983); 4—Druffel (this work); 5—Druffel (1981); 6—Konishi *et al.* (1981); 7—Bien and Suess (1967).]

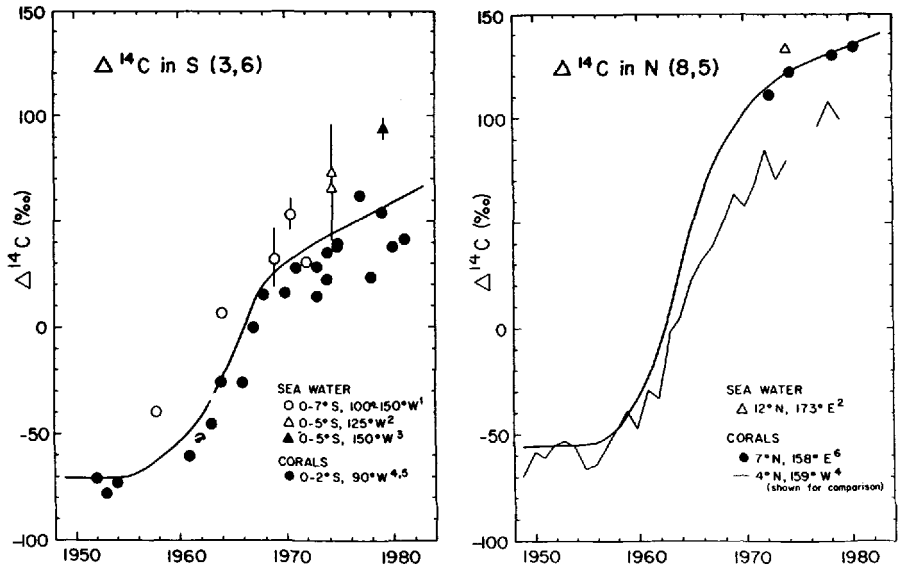

Figure 9. (Continued)

the radiocarbon trends, which were fit by hand to the data. Two of the trends are based on limited data. Pre-1970 $\Delta^{14}C$ values for the $N(8, 5)$ flow are taken to be slightly elevated with respect to coral results at Fanning Island, which lies 3° closer to the equator. The $\Delta^{14}C$ trend in the $W(11, i)$ flows is devoid of data from 1960–1971, and thus has been assigned an average depletion of about 40‰ with respect to overlying waters during this period. The impact of this assumption on our model calculations is analyzed below.

Eq. (2) and (3) are solved using a 0.1 year time interval for the period 1955–1982. The resultant $\Delta^{14}C$ time histories calculated for boxes 5 and 6 are presented in Figure 10 a and b, respectively. The agreement is good between the calculated trends and the actual measurements, indicating that the flow assignments and $\Delta^{14}C$ time histories adequately define the $\Delta^{14}C$ in boxes 5 and 6. Prior to 1960, the $\Delta^{14}C$ trend in box 5 is slightly lower than the measured values which, as discussed above, may suggest the early arrival of bomb radiocarbon in the tropical Pacific prior to that in other areas farther from ground level testing sites in the Marshall Islands during 1952–1954. It is anticipated that $\Delta^{14}C$ values for pre-1960 Canton coral bands will reveal the same or greater disparity, due to its proximity to the Marshall Islands testing sites.

Sensitivity of the annual model to the South Equatorial Current input, which constitutes about 20% of the total flow into boxes 5 and 6, is illustrated in Figure 10a and b. The model was run with $S(2, 5)$ and $S(3, 6)$ equal to zero and double the original values. There is relatively good agreement with the pre-1970 measurements in box 5, but higher values are predicted subsequent to 1972 when $S(2, 5) = 0$ (Fig. 10a).

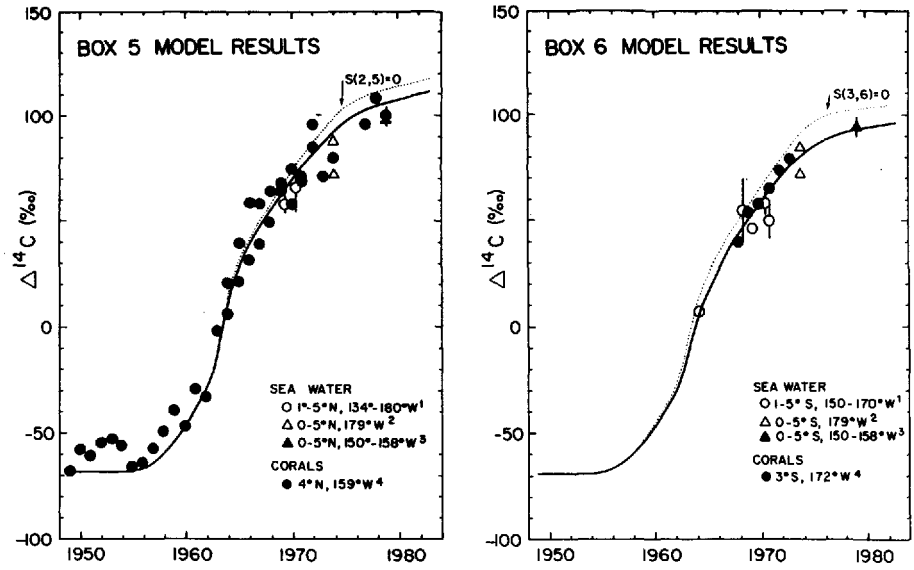

Figure 10. Time histories of $\Delta^{14}C$ at (a) Fanning Island (box 5) and at (b) Canton Island (box 6). The points represent measured values in sea water and in banded corals, the solid lines are trends calculated using the annual version of the model and the dashed lines are model-calculated trends where $S(2, 5) - S(3, 6) = 0$. [References same as in Fig. 9.]

$S(3, 6)$ appears more important for describing the radiocarbon in box 6 as >90% of the observed values lie below the $S(3, 6) = 0$ curve. Regardless, the shift of the predicted trends is relatively minor when $S(2, 5)$ and $S(3, 6)$ are either doubled or eliminated. This is in general agreement with the previous studies of Wyrtki (1981) and Quay *et al.* (1983) that show the major input of water on an annual basis to the equatorial Pacific is meridional transport of higher latitude waters via geostrophic transport.

The sensitivity of the model to the uncertainty in the $\Delta^{14}C$ trend in upwelling water is tested by running the model using $\Delta^{14}C$ values that are ±20‰ for the period 1960–1971 in Figure 9c. Using these bounds, model calculated $\Delta^{14}C$ trends for both boxes 5 and 6 changed by less than ±6‰, which demonstrates that the uncertainty in the $\Delta^{14}C$ trend for upwelling water does not significantly change the results of our model calculations.

To test the model results, equatorial distributions of tritium, total inorganic carbon concentration (ΣCO_2) and salinity are examined. From the distribution of tritium in the tropical Pacific, Fine *et al.* (1987) concluded that tritium in the upper ocean reflects advection of water via the mean wind-driven circulation along isopycnal surfaces spreading from their winter time outcrops. The agreement between observed tritium distributions and those calculated using the model reflects the ability of the model to reproduce the actual flow fields in the tropical Pacific. ΣCO_2 concentrations measured during GEOSECS will provide a test of the model assumption that states the

Table 3. Average values for tritium, ΣCO_2 and salinity from various authors for tests of the model. See text for detail.

Flow	Tritium [T.U.]	ΣCO_2 [mol/m^3]	Salinity [‰]
G(4,5)	3.7	2.008	35.04
G(7,6)	2.9	2.025	35.25
W(11, 5 or 6)	2.0	2.042	35.34
S(2,5)	2.7	2.014	35.23
S(3,6)	3.0	2.042	34.97
N(8,5)	2.8	1.988	34.77
Box 5	2.5	2.011	35.17
Box 6	2.2	2.027	35.48

cycling of inorganic carbon in the tropical Pacific is controlled primarily by advective processes, namely geostrophic transport, Ekman divergence and zonal currents. Salinity, like tritium, displays a north-to-south gradient that should be reproduced by the annual model.

Average tritium concentrations during 1973–1982 for each of the boxes described in the model are listed in Table 3. A steady state is assumed, as tritium concentrations appear to have remained constant during the period of observations (Fine *et al.*, 1987). Using the flow fields established above for the ^{14}C data, the tritium values calculated for boxes 5 and 6 are 2.4 and 2.0 T.U., respectively. Average values obtained from Fine *et al.* (1987, their Fig. 8) are 2.5 T.U. in box 5 and 2.2 T.U. in box 6. The agreement between the observed and calculated values is an indication that similar mixing processes control the distribution of tritium and bomb radiocarbon.

Average estimates of ΣCO_2 have been calculated from Geosecs data (Broecker *et al.*, 1982) for each of the boxes in the model (Table 3). As ΣCO_2 values have probably not changed significantly during the time frame of the model, steady state ΣCO_2 was calculated using Eqs. (2) and (3); this results in ΣCO_2 values of 2.020 μM/kg in box 5 and 2.035 μM/kg in box 6. Average values for boxes 5 and 6 obtained from Geosecs data in the upper 80 m of the water column are 2.011 and 2.027 μM/kg, respectively. The model calculated values are 8–9 μmoles/kg higher than the observed values, which most likely represents CO_2 lost to the atmosphere at the equator. The partial pressure of CO_2 in surface sea water near the equator is much higher (by 60 p.p.m.v.) than that in the atmosphere, which is maintained by upwelling of subsurface waters that have undergone considerable oxidation of organic matter. This estimate of CO_2 loss to the atmosphere is less than that calculated by Broecker and Peng (1982) based on nitrate deficiencies in the surface waters, but this may be due to different boundary conditions used for the two sets of calculations.

A final test of the model results is obtained using salinity distributions. Average salinity values were calculated (Table 3) for each of the boxes in the model from the same Geosecs stations used to calculate the average ΣCO_2 values. The salinity values

calculated for boxes 5 and 6 are 35.11 and 35.28‰, respectively, where the observed average values are 35.17 and 35.48‰. The agreement between calculated and observed values is good for box 5; however, there is a considerable discrepancy between those values for box 6. This is most likely caused by external controls on surface salinity, that is, the difference between evaporation and precipitation. At the equator and to the south, evaporation exceeds precipitation (Dietrich *et al.*, 1963), which would cause the average salinity in box 6 to be greater than that calculated using the model, in agreement with the model results. In the vicinity of box 5 precipitation either equals or exceeds evaporation, and is consistent with the good agreement between calculated and observed values. Though constrained by limitations on the data set, the results of these tests strengthen the confidence in the annual flow model developed above.

b. Seasonal model. Inputs to the model are now changed to represent actual seasonal variations for the period 1970–1975. The flow fields for the seasonal model are reassigned so that they conform to the seasonally changing wind field. Figure 11a to e shows the change of each of the flows used in the model on a seasonal basis. Geostrophic convergence $G(i, j)$ does not vary over the course of a year, as a strong difference of the east to west slope of the thermocline between 5N and 5S (from which $G(i, j)$ values are calculated) is difficult to generate (Wyrtki, 1981). Trans-equatorial Ekman transport of about 6.5×10^6 m^3s^{-1} from summer to winter hemisphere (Wyrtki, 1981) causes a factor of two seasonal variation in the $W(11, 5)$ and $W(11, 6)$ flows (Fig. 11c and d). The North Equatorial Counter Current flow into box 5 achieves its maximum flow during November–January ($N(8, 5)$ - 4×10^6 m^3s^{-1}) and is near zero during May–June (Taft and Kovala, 1981; Taft *et al.*, 1982a, b).

Figure 12a to f shows the change of $\Delta^{14}C$ in each of the flows used in the seasonal model. It seems unlikely that $\Delta^{14}C$ varied seasonally in $G(i, j)$ based on minimal changes in mixed layer depth that occur seasonally. However, the strong seasonality of the North Equatorial Countercurrent flow into box 4 (highest during May–June) could conceivably cause a maximum of $\Delta^{14}C$ during mid-year of 10–15‰ (Fig. 12a). As the geostrophic flow of water into the subsurface box does not vary seasonally (Wyrtki, 1981), it is assumed that the $\Delta^{14}C$ of the upwelling waters similarly does not change with season. A seasonal variability of 15–20‰ has been superimposed on the $S(2, 5)$ and $S(3, 6)$ $\Delta^{14}C$ trends, in accord with seasonal $\Delta^{14}C$ results observed in Galapagos corals (Druffel, 1981). The effects of these assumptions on the model results is included in the error analyses below.

Eqs. (2) and (3) are solved for various values of $S(2, 5)$ and $S(3, 6)$ until the correct values for the seasonal $\Delta^{14}C$ variation in boxes 5 and 6, respectively, are obtained. The time interval used for the seasonal model is also 0.1 years. Best-fits of the Fanning and Canton coral data were sought on the basis of the observed seasonal variations during non-ENSO periods, which were 12 ± 4‰ and 25 ± 5‰, respectively. Using these criteria, a best-fit of the Fanning coral data was achieved when $S(2, 5)$ varied from

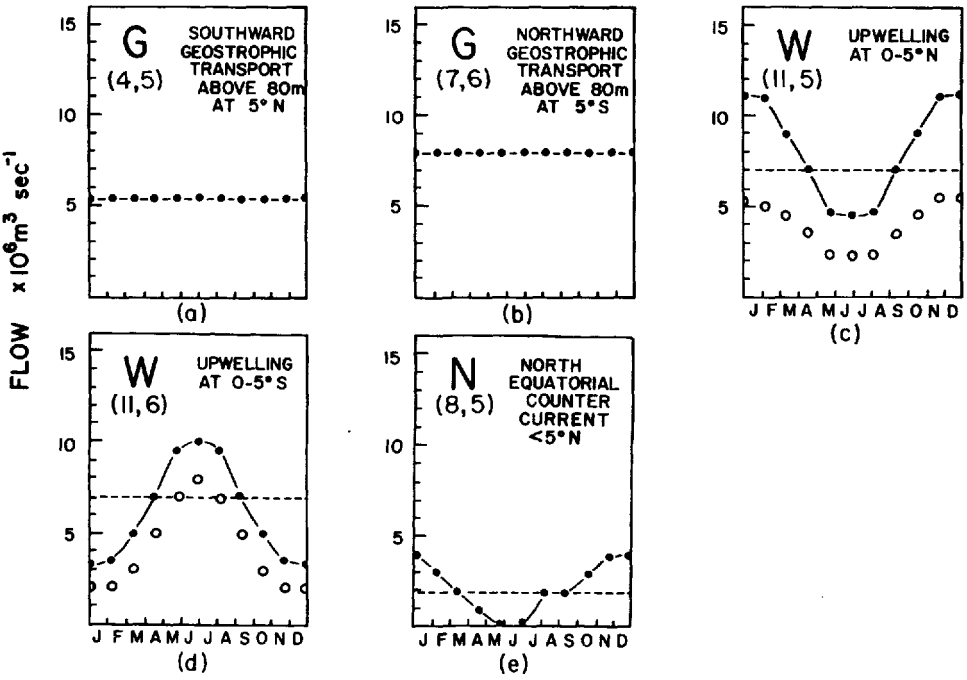

Figure 11a-e. Water flows of the various currents and water masses into boxes 5 and 6 used in the seasonal model. Dashed lines represent the flows used in the annual model. Open circles reflect reduction in upwelling during ENSO events.

4.5×10^6 m^3s^{-1} to 0.5×10^6 m^3s^{-1}, and that for the Canton data was obtained when $S(3, 6)$ varied from 7×10^6 m^3s^{-1} to 1×10^6 m^3s^{-1} (Fig. 13a and b).

The model calculated $\Delta^{14}C$ trends appear as solid lines in Figure 14a and b. The error bands shown are determined by assigning an error of ±15% to the $G(i, j)$, $S(i, j)$, $W(11, i)$ and $N(8, 5)$ flows, and an error of ±5‰ to the $\Delta^{14}C$ values shown in Figure 12a to e. Coral that accreted during or just subsequent to the '69–'70 and '72–'73 ENSO events appear higher in $\Delta^{14}C$ than the model prediction, due to the interruption of normal flow patterns.

Sensitivity analyses reveal that the timing of the $\Delta^{14}C$ peaks and troughs is most sensitive to the seasonality of the transequatorial Ekman transport, which funnels 2–3 times more upwelled water of low $\Delta^{14}C$ during winter. By 1974, the variation of the seasonal $\Delta^{14}C$ signal in box 5 is virtually gone, due in part to the fact that the bomb radiocarbon signatures of the various inputs approach a common value.

The seasonal variation of $\Delta^{14}C$ in box 5 is clearly less than that for box 6, because two sources of ^{14}C-poor water to box 5, $S(2, 5)$ and $W(11, 5)$, are at their maximum flows during opposing seasons, which causes a damping of the seasonal signal. In contrast, $S(3, 6)$ and $W(11, 6)$ are at their maximum flows during southern winter, which results in very low $\Delta^{14}C$ values during mid-1971. The coupling of low ^{14}C flows

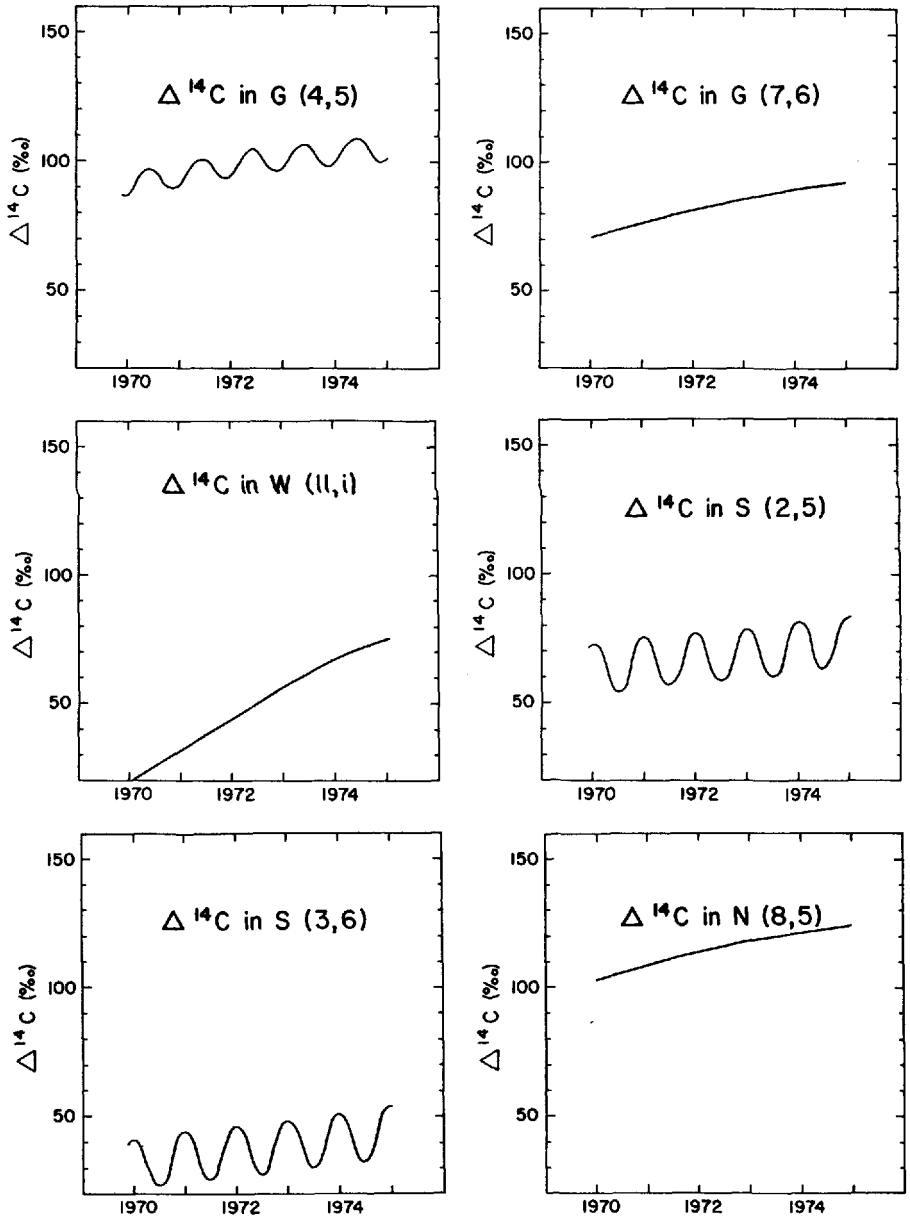

Figure 12a-f. Time histories of $\Delta^{14}C$ from 1970–1975 in the various currents and water masses used in the seasonal model.

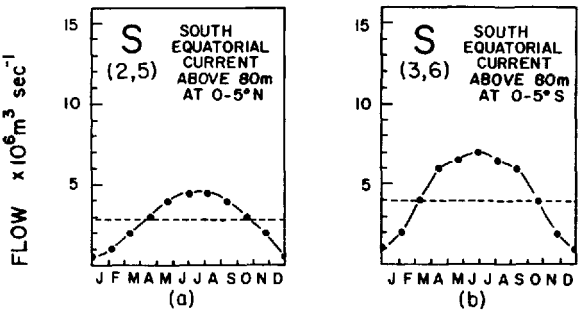

Figure 13. Seasonal model calculated water flows from the South Equatorial Current into (a) box 5 and (b) box 6. See text for details.

during the same season is the reason that the seasonal variation of $\Delta^{14}C$ in box 6 decreases only slightly by 1975.

The sensitivity of the model to the $S(2, 5)$ and $S(3, 6)$ flows is examined by setting these parameters equal to zero and to a constant value year round. If $S(2, 5)$ and $S(3, 6)$ were zero, model calculated $\Delta^{14}C$ values in boxes 5 and 6 would be too high by 10–15‰, and the resultant seasonal variations equal in both boxes (~17‰). Similarly, if $S(2, 5)$ and $S(3, 6)$ were constant year round, seasonal variations would be equal in boxes 5 and 6 (16–17‰). Thus, it is critical to know whether the difference in the seasonal $\Delta^{14}C$ signal at Fanning is significantly different from that at Canton. It is clear that the data sets from which I am basing this argument are very small, only one and one-half years and four points for each site. However, it appears from these limited data that the seasonal signal at Fanning (12 ± 4‰) is smaller than that at Canton (25 ± 5‰), and based on this assumption, model results indicate that the South Equatorial Current flow varies seasonally. Transequatorial Ekman transport from summer to winter hemisphere alone is apparently not sufficient for defining the observed seasonal variations in bomb radiocarbon. Extension of these data sets must be achieved to confirm this result.

The major conclusion from these modelling exercises is that annual and seasonal $\Delta^{14}C$ trends are satisfactorily reproduced using a well-constrained system with independently established flow fields. The time-dependent, advective three-dimensional box model appears adequate to explain the cycling of carbon in the tropical Pacific. On an annual basis, radiocarbon in the tropical mid-Pacific is affected to a minor extent by the South Equatorial Current in agreement with previous studies. However, observed seasonal variations in the $\Delta^{14}C$ signal near the equator appear to be controlled by variation in the flow of the South Equatorial Current.

Acknowledgments. Many thanks to Sheila Griffin, whose dedication and skill in setting up and running the WHOI Radiocarbon Lab has been the main reason for its success. I thank Stephen Smith, Randi Schneider, Peter Glynn, Gerry Wellington, Gary Robinson, J. Robbie

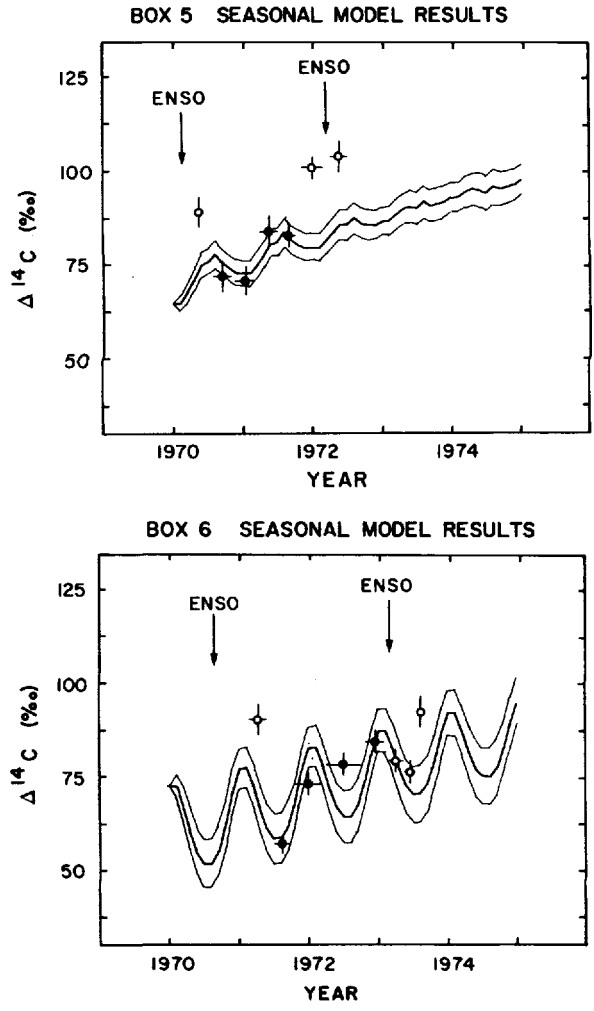

Figure 14a-b. Seasonal variation of $\Delta^{14}C$ in surface waters in (a) box 5 and (b) box 6. Observed values are shown by filled circles (non-ENSO growth) and open circles (ENSO growth). The error bands shown are determined by assigning an error of ±15% to the various flows and an error of ±5‰ to the $\Delta^{14}C$ trends shown in Figure 12a to f.

Toggweiler and Bill Moore for providing the coral samples. John A. Frankenthal provided excellent technical assistance. Robert Buddemeier, J. Robbie Toggweiler, George Veronis, Ted Foster, and two anonymous reviewers offered constructive comments of the manuscript. Thanks to Margaret Harvey, and Molly Lumping for preparing the manuscript and to Sheila Griffin for drafting the figures. This work was funded by the National Science Foundation through grants OCE81-11954 and OCE83-15260. This is Woods Hole Oceanographic Institution Contribution No. 5978.

REFERENCES

Bien, G. and H. Suess. 1967. Transfer and exchange of C-14 between the atmosphere and the surface water of the Pacific Ocean, radioactive dating and methods of low level counting, IAEA Vienna, 105–115.

Broecker, W. S. and T. S. Peng. 1980. Seasonal variability in the $^{14}C/^{12}C$ ratio for surface ocean water. Geophys. Res. Lett., *7,* 1020–1022.

—— 1982. Tracers in the Sea, Lamont-Doherty Geological Observatory, Columbia University, Palisades, NY, 427–429.

Broecker, W. S., T-H. Peng, G. Ostlund and M. Stuiver. 1985. The distribution of bomb radiocarbon in the ocean. J. Geophys. Res., *90,* 6953–6970.

Broecker, W. S., D. W. Spencer and H. Craig. 1982. Geosecs Pacific Expedition, Hydrographic Data, Vol. 3, U.S. Government Printing Office, Washington, DC, 137 pp.

Bryden, H. L. and E. C. Brady. 1985. Diagnostic model of the three-dimensional circulation in the upper equatorial Pacific Ocean. J. Phys. Oceanogr., *15,* 1255–1273.

Burling, R. W. and D. M. Garner. 1959. A section of ^{14}C activities of sea water between 9°S and 60°S in the Southwest Pacific Ocean, New Zealand, J. Geol. Geophys., *2,* 799–824.

Cain, W. F. and H. E. Suess. 1976. Carbon-14 in tree rings. J. Geophys. Res., *81,* 3688–3694.

Chave, K. E. and E. A. Kay. 1973. Fanning Island Expedition, July and August 1972, HIG Report 73-13, University of Hawaii at Manoa.

Dietrich, G., K. Kalle, and F. Ostapoff. 1963. General Oceanography. An Introduction. John Wiley and Sons, NY, 186–190.

Druffel, E. M. 1981. Radiocarbon in annual coral rings from the eastern tropical Pacific Ocean. Geophys. Res. Lett., *8,* 59–62.

—— 1985. Detection of El Niño and decade timescale variations of sea surface temperature from banded corals: Implications for the carbon dioxide cycle. AGU Monographs, Proc. Chapman Conf. on Atmospheric CO_2, Tampa, 9–13 January 1984.

Druffel, E. M. and T. W. Linick. 1978. Radiocarbon in annual coral rings of Florida. Geophys. Res. Lett., *5,* 913–916.

Dunbar, R. B. and G. M. Wellington. 1981. Stable isotopes in a branching coral monitor seasonal temperature variation. Nature, *93,* 453–455.

Eastropac Atlas. U.S. Dept. Comm. NOAA, Nat. Mar. Fisheries Serv., Cuthbert M. Love, ed., circular 330, volumes 2 (1971), 1, 5, 6 (1972), 9, 10 (1975).

Emanuel, W. R., G. G. Killough, W. M. Post, H. H. Shugart and M. P. Stevenson. 1984. Computer implementation of a globally averaged model of the world carbon cycle, DOE Document No. DOE/NBB-0062, UC-11, 79 pp.

Fairbanks, R. G. and R. E. Dodge. 1979. Annual periodicity of $^{18}O/^{16}O$ and $^{13}C/^{12}C$ ratios in the coral *Montastrea annularis.* Geochim. Cosmochim. Acta, *43,* 1009–1020.

Federal Radiation Council. 1963. Estimates and evaluation of fallout in the United States from nuclear weapons testing conducted through 1962. Rep. No. *4,* 31 pp.

Fine, R. A., W. H. Peterson and H. G. Ostlund. 1987. The penetration of tritium into the tropical Pacific, J. Phys. Oceanogr., *17,* 553–564.

Firing, E. 1981. Current profiling in the NORPAX Tahiti Shuttle, Trop. Ocean-Atmos. Newslett., *5.*

Knutson, D. W., R. W. Buddemeier and S. V. Smith. 1972. Coral chronometers: seasonal growth bands in reef corals. Science, *177,* 270–272.

Konishi, K., T. Tanaka and M. Sakanoue. 1981. Secular variation of radiocarbon concentration in sea water: sclerochronological approach, Proc. of the Fourth Inter. Coral Reef Symposium, Manila, v. I, 181–185.

Levin, I., B. Kromer, H. Schoch-Fischer, M. Bruns, M. Munnich, D. Berdan, J. C. Vogel and K. O. Munnich. 1985. 15 years of tropospheric ^{14}C observations in Central Europe. Radiocarbon, *27,* 1–19.

Linick, T. W. 1978. La Jolla measurements of radiocarbon in the oceans. Radiocarbon, *20,* 333–359.

—— 1980. Bomb-produced carbon-14 in the surface water of the Pacific Ocean, *in* Internat'l Radiocarbon Conf., 10th Proc., Stuiver, M. and R. S. Kra, eds., Radiocarbon, *22,* 599–606.

Nozaki, Y., D. M. Rye, K. K. Turekian and R. E. Dodge. 1978. C-13 and C-14 variations in a Bermuda coral. Geophys. Res. Lett., *5,* 825–828.

Nydal, R. and K. Loveseth. 1983. Tracing bomb ^{14}C in the atmosphere. J. Geophys. Res., *88,* 3621–3646.

Ostlund, H. G., R. Brescher, R. Oleson and M. J. Ferguson. 1979. GEOSECS Pacific Radiocarbon and Tritium Results (Miami), R.S.M.A.S. Tritium Laboratory Data Report #8, 171 pp.

Ostlund, G. and M. Stuiver. 1980. GEOSECS Pacific Radiocarbon. Radiocarbon, *22,* 25–45.

Quay, P. D., M. Stuiver and W. S. Broecker. 1983. Upwelling rates for the equatorial Pacific Ocean derived from the bomb ^{14}C distribution. J. Mar. Res., *41,* 769–793.

Reid, J. L. 1968. On the circulation, phosphate-phosphorous content and zooplankton volumes in the upper part of the Pacific Ocean. Limnol. Oceanogr., *7,* 287–306.

Richards, A. F. 1957. Volcanism in eastern Pacific Ocean basin, 1954–1955, Intern. Geol. Congress, Mexico, Proc. X, *1,* 19–31.

Stuiver, M. and H. A. Polach. 1977. Reporting of ^{14}C data. Radiocarbon. *19,* 355–363.

Taft, B. A., A. Cantos-Figuerola and P. Kovala. 1982a Vertical sections of temperature, salinity, thermosteric anomaly and zonal geostrophic velocity from NORPAX shuttle experiment—Part 3, NOAA Data Report ERL PMEL-7, 92 pp.

Taft, B. A. and P. Kovala. 1981. Vertical sections of temperature, salinity, thermosteric anomaly and zonal geostrophic velocity from NORPAX shuttle experiment, Part-1, NOAA Data Report ERL PMEL-3, 98 pp.

Taft, B. A., P. Kovala and A. Cantos-Figuerola. 1982b. Vertical sections of temperature salinity, thermosteric anomaly, and zonal geostrophic velocity from NORPAX shuttle experiment—Part 2, NOAA Data Report ERL PMEL-5, 94 pp.

Toggweiler, J. R. and S. Trumbore. 1985. Bomb-test 90Sr in Pacific and Indian Ocean surface water as recorded by banded corals. Earth Planet. Sci. Lett. *74,* 306–314.

Weber, J. N. and P. M. J. Woodhead. 1972. Temperature dependence of oxygen-18 concentration in reef coral carbonates. J. Geophys. Res., *77,* 463–473.

Weil, S. M., R. W. Buddemeier, S. V. Smith and P. M. Kroopnick. 1981. The stable isotopic composition of coral skeletons: control by environmental variables. Geochim. Cosmochim. Acta, *45,* 1147–1153.

Williams, D. F., M. A. Arthur, D. S. Jones and N. Healy-Williams. 1982. Seasonality and mean annual sea surface temperatures from isotopic and sclerochronological records. Nature, *296,* 432–434.

Wyrtki, K. 1975. El Niño—dynamic response of the equatorial Pacific Ocean to atmospheric forcing. J. Phys. Oceanogr., *5,* 342–584.

—— 1981. An estimate of equatorial upwelling in the Pacific. J. Phys. Oceanogr., *11,* 1205–1214.

Wyrtki, K. and B. Kilonsky. 1984. Mean water and current structure during the Hawaii-to-Tahiti shuttle experiment. J. Phys. Oceanogr., *14,* 242–254.

Received *24 June, 1985;* revised: *2 June, 1987.*